Polymer Vol. 39 No. 23, pp. 5633–5642, 1998
0032-3861/98/$ – see front matter

PII: S0032-3861(98)00096-2

Viscosity difference as distributing factor in selective absorption of aluminium borate whiskers in immiscible polymer blends

Anders L. Persson and Hans Bertilsson*
Department of Polymeric Materials, Chalmers University of Technology, S-412 96 Göteborg, Sweden
(Received 15 May 1997; revised 27 October 1997; accepted 8 January 1998)

The distribution of aluminium borate whiskers in blends of polyethylene/polyisobutylene (PE/PIB) was studied with respect to viscosities of the components. Both polymers are non-polar with slightly higher surface energy for the PE, i.e. weak filler–polymer interactions of about equal strength. The significance of the polymers' viscosity disparity can thus be studied in isolation. Two PEs and two PIBs with clearly separated flow curves ($\eta_{PE1} > \eta_{PIB1} \gg \eta_{PE2} > \eta_{PIB2}$) were used. The whiskers were found in the high viscosity phase except when they promoted coherency of the low viscosity minority phase. However, the PE's slightly higher surface energy ruled the absorption although PIB was slightly more viscous showing the relative weakness of this rheological phenomenon. Furthermore, the viscosity distributing factor was found to be less important than polar interactions. A rheological explanation is presented that supports the observed selective absorption.

(Keywords: filled polyolefin blends; co-continuity; rheology)

INTRODUCTION

Filled polymer blends constitute a group of materials that is gaining interest, both from technical and academic considerations[1–7]. Phase morphology can be controlled by introducing a solid into a polymer blend, however, there are several inherent difficulties that need to be mastered to achieve an attractive property profile. Among them are the polymers' mutual interactions and the strength of their individual interactions with the solid surface. Furthermore, the parameters that control the morphology of unfilled blends set the starting constraints for the three-component systems. Most important are the volume and viscosity ratios of the polymers and their elasticities.

Our previous reports[5–7] have concerned polymers with strong interactions with filler surfaces. During injection moulding the morphologies created during compounding were ruined[6]. Also the beneficial selective adsorption in electrically conducting blends that only provided marginal improvement[7] have stressed the need for this investigation. In contrast to previous work[5–7] the current project was concerned with how the rheology of the polymer components influences the whisker distribution in blends with marginal polymer–solid interactions. Thus two grades of polyethylene (PE) and two grades of polyisobutylene (PIB) were chosen. According to Wu[8] the surface tensions of PE and PIB at 180°C are 26.5 and 23.4 mN^{-1}, respectively, which should ensure a very low interfacial tension that could be important considering the energetic step required for a filler particle to move across the interface.

This blend is not purely of academic interest. According to the PIB manufacturers, the properties of polyolefins (PE, PP) are improved by small additions of PIB. These properties include the impact strength, the tear strength, barrier properties, the flexibility and the stress cracking resistance. However, the tensile strength and stiffness are inferior to the pure polyolefin. Addition of filler may balance these shortcomings.

Concerning the composite formulations, two main aspects had to be considered. Firstly, to reduce the influence of the filler itself whisker contents were chosen sufficiently low to avoid filler particle percolation in any of the phases, even considering that the minority phase might absorb all the whiskers. According to Chmutin *et al.*[9] the percolation should occur at 17 volume % (v/o) for an aspect ratio of 27. From the work of Bigg[10] a stricter percolation threshold can be found, at 7 v/o. We used 5 v/o maximum whisker loading to avoid percolation. Secondly, we have found the whiskers to promote co-continuity[5–7]. To minimize this effect the polymer volume fractions (ϕ_1 and ϕ_2) were chosen primarly according to the expression by Jordhamo and co-workers[11] (equation (1)), since this expression has been shown to predict the point of phase inversion in several cases. η_1 and η_2 denote the viscosities of the two polymers.

$$\frac{\eta_1}{\eta_2} \cdot \frac{\phi_2}{\phi_1} = 1 \qquad (1)$$

For an already co-continuous blend the whiskers move from one continuous phase to the other. In this way the morphological influence of the whiskers is minimized.

Master batches of whisker filled single plastic composites were prepared and the complementary plastic was added in a second step. Thus any effect of the origin matrix on whisker distribution could be studied.

The polymers were rheologically characterised in a plate–plate rotational rheometer run in harmonic mode. The interfacial tension between PE and PIB in the molten state was measured by the imbedded disc retraction

* To whom correspondence should be addressed (fax: +46-31-7721313; e-mail: hansb@polymm.chalmers.se)

Table 1 Characteristics of used materials

Material	M_n (kg mol^{-1})	M_w (kg mol^{-1})	M_v (kg mol^{-1})	MFI (g per 10 min)
PE1	24	300		2, 190°C, 21.6 kg
PE2	17	54		15, 190°C, 2.16 kg
PIB1	38	384	400	
PIB2	12	101	85	
SAN				0.3, 200°C, 5 kp[a]
PA6			18[a]	

[a]Provided by the supplier.

method[12]. All blends and composites were compounded in a batch mixer and their morphologies were studied by scanning electron microscopy. The rheology of the composites and blends was studied in a rotational rheometer with cone–plate to assure uniform shear rate throughout the sample.

EXPERIMENTAL

The materials used were two high density grade polyethylenes, Lupolen 5261 (PE1) and DMDS 7015 (PE2) from Borealis and two polyisobutylenes from Scientific Polymer Products, (PIB1) and (PIB2). Their molecular mass distributions were determined by size exclusion chromatography with polyethylene and polystyrene standards in 1,2,4-trichlorobenzene and tetrahydrofurane for PE and PIB, respectively. A poly(ϵ-caprolactam), (PA6), Ultramid B3 and a poly(styrene-co-acrylonitrile), (SAN), Luran 388S with 35% acrylonitrile content were provided together with the Lupolen by BASF. Aluminium borate whiskers $(Al_2O_3)_9(B_2O_3)_2$, Alborex G, are single crystals with diameters of 0.5–1 μm, lengths of 10–30 μm, a density of 2.93 g cm^{-3} and a specific surface area of 2.5 m^2 g^{-1}. The whiskers have excellent mechanical properties as well as thermal and chemical stability. They were provided by Shikoku Chemicals Corp. The densities at 170°C are 0.774, 0.717 and 2.92 g cm^{-3} for PE, PIB and whiskers, respectively. The characteristics of the materials used can be found in *Table 1*.

Compounding of the polyolefin blends and composites was done in a 50 cm^3 Brabender AEV 330 plasticorder at 170°C and 50 rpm for about 5 min. Identical conditions were used for the SAN/PA6-W composites except that the temperature was 235°C. The high viscosity polymer was first put into the compounding chamber and was completely

Table 2 Compounded blends and composites. The volume fractions in column three refer to the molten state at 170°C, e.g. C7 consists of 11.4 v/o PIB1 and 0.5 v/o whiskers precompounded into the PIB and 88.1 v/o PE1

	Ingredients	(vol/vol)	m_{PIB} (g)	m_{PIB+W} (g)	m_{PE} (g)	m_{PE+W} (g)	m_W (g)
B1	PIB1/PE1	53.6/46.4	20.72		19.35		
B2	PIB1/PE1	27.7/72.3	10.36		29.02		
B3	PIB1/PE2	53.6/46.4	20.72		19.35		
B4	PIB1/PE2	73.0/27.0	20.02		11.61		
B5	PIB2/PE2	53.6/46.4	20.72		19.35		
B6	PIB2/PE2	38.4/61.6	14.51		25.15		
B7	PE1/PE2	2.5/97.5			0.97/37.73		
B8	PIB1/PIB2	15.0/85.0	6.22/35.23				
C1	PIB1-W	95.6-4.4	39.38				7.32
C2	PIB2-W	95.6-4.4	39.38				7.32
C3	PE1-W	95.0-5.0			36.76		7.32
C4	PE2-W	95.0-5.0			36.76		7.32
C5	C1/PE1	52.6(2.3)/45.1		23.95	18.85		
C6	C1/PE1	27.6(1.2)/71.2		12.13	28.64		
C7	C1/PE1	11.4(0.5)/88.1		4.89	34.65		
C8	PIB1/C3	52.2/45.5(2.3)	20.19			22.61	
C9	PIB1/C3	26.7/69.8(3.5)	10.23			34.36	
C10	C1/PE2	52.6(2.3)/45.1		23.95	18.85		
C11	C1/PE2	70.8(3.1)/26.1		33.19	11.20		
C12	C1/PE2	32.8(1.4)/65.8		18.08	33.21		
C13	C1/PE2	11.4(0.5)/88.1		4.89	34.65		
C14	PIB1/C4	32.8/65.8(1.4)	15.24			36.04	
C15	PIB1/C4	52.2/45.5(2.3)	20.19			22.61	
C16	PIB1/C4	67.6/30.9(1.5)	27.98			16.40	
C17	C2/PE2	52.6(2.3)/45.1		23.95	11.20		
C18	C2/PE2	37.9(1.7)/60.5		16.90	24.70		
C19	PIB2/PE2-W	66.9/30-3.1	22.98		11.61		4.53
C20	PIB2/C4	52.2/45.5(2.3)	20.19			22.61	
C21	PIB2/C4	37.0/60.0(3.0)	14.03			29.17	
C22	B7/B8-W	45.3/52.3-2.4	20.19		18.86		3.75
C23	SAN/PA6-W		24.36[a]		24.36[b]		3.75

[a]Mass of PA6.
[b]Mass of SAN.

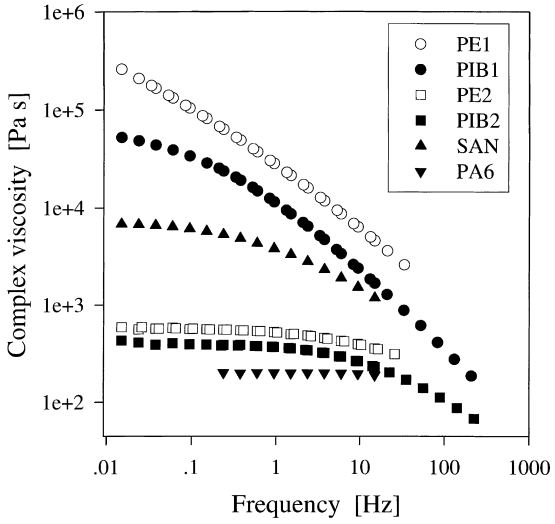

Figure 1 Rheological behaviour from rotational rheometer runs of the plastics utilized. The rheometer was run in harmonic mode at 170 and 100°C (curve shifted to 170°C) for the PIBs and 170 and 140°C (curve shifted to 170°C) for the PEs. SAN and PA6 were run at 235°C

molten before the second polymer was added. The whisker fraction of the filled blends were added from the precompounded single-polymer composites (C1–C4) that carried up to 5 v/o whisker loading. For example, C11 in *Table 2* was prepared by compounding 33.19 g of C1 with 11.20 g of PE2. However, among the composites and blends in this work C19, C22 and C23 are exceptions to this rule. For these composites the whiskers were added to molten blends as indicated in *Table 2*.

Rheological characterisation of the polymers and single polymer composites was performed in a Rheometrics RDA II with parallel plates of 25 mm diameter in dynamic mode. A cone and plate geometry was utilised for steady shear experiments. The PIBs were run at 170 and 100°C and PE at 170 and 140°C; all other runs were performed at 170°C. The samples were heated at 170°C for 4 min and then deformed to the required circular shape. After this they were left at rest for 10 min before any shearing took place.

Interfacial tension between PE and PIB was measured by the imbedded disc retraction method on the PE2–PIB2 at 150°C and at 170°C for PE2–B8. The discs were prepared from compression moulded PE2-films of 50–80 μm thickness. All samples were conditioned at 120°C for more than 90 min before the run. For a comprehensive description of the experimental procedure see Rundqvist *et al.*[12].

Scanning electron microscopy (SEM) was done on a Zeiss DSM 940A. Samples were prepared by cryofracturing the compounds. Extraction of the PIB phase was accomplished by several consecutive immersions of the sample in cyclohexane followed by gold-sputtering of the residue. Unless otherwise stated, all micrographs originate from Brabender compounded samples.

Pyrolysis of the polymer content was done at 500°C on samples that had been PIB-extracted and centrifuged.

RESULTS AND DISCUSSION

The viscosities of the pure polymers are presented in *Figure 1*. The flow curves of the polyolefins are clearly separated for the current shear rates. Accordingly, the blends and composites in *Table 2* are comprised of viscously distinguishable phases during their compounding.

The interfacial tension between PIB-W and PE-W needed to be quantified to isolate the influence of the viscous distributing factor. However, they are not easily accessible. Determination of the polymers' interfacial tension, γ_{23}, shows if they have different surface tensions, γ_2 and γ_3, that determine their individual interfacial tension with the whiskers, γ_{12} and γ_{13}. The whisker surface is a high-energy surface[6] which attracts the polymer of the highest specific surface energy in order to minimize the total interfacial energy of the three-component system. The polymer's interfacial tension can be directly measured using the imbedded disc retraction method[12]. It can also be calculated using the harmonic mean equation[8] which is valid for low-energy materials such as our polyolefins. A comprehensive discussion on arguments for the harmonic mean equation in favour of the geometric mean approximation is presented in Wu's textbook[8]. For our non-polar polymers the harmonic mean approach gives:

$$\gamma_{23} = \gamma_2 + \gamma_3 - \frac{4\gamma_2\gamma_3}{\gamma_2 + \gamma_3} \tag{2}$$

Wu[8] also provides experimental data on the surface tensions of linear PE (γ_{PE}) and PIB (γ_{PIB}) and the widely recognized expressions on how they relate to temperature

$$\gamma = \gamma_0 \left(1 - \frac{T}{T_C}\right)^{11/9} \tag{3}$$

and molecular mass

$$\gamma = \gamma_\infty - \frac{k_e}{M_n^{2/3}} \tag{4}$$

where γ_0 is the surface tension at zero Kelvin and T_C is the critical temperature, γ_∞ is the surface tension for a sample of infinite molecular mass and k_e is a material specific empirical constant. *Table 3* presents γ_{23} for the plastics used in this study calculated according to equation (2). The calculated γ_2 and γ_3 from equation (4) of our grades are valid at 20 and 24°C for PE and PIB, respectively. To get the desired interfacial tension at 170°C, the constants γ_0 and T_C in equation (3) have to be modified. If we first assume that γ_0 does not

Table 3 Interfacial tension of utilized polyolefin pairs according to equation (2). γ_{23} in column 2 is based on γ_2 and γ_3 from equation (3) with γ_0 and T_C from Wu's literature data. Columns 3 and 4 show the surface tensions that are based on the actual M_n values calculated for room temperature and using the recalculated equation (3) with either γ_0 or T_C from the literature[8]. Data from imbedded disc retraction measurements are shown in column 5 with the standard deviation specified

Materials	γ_{23}, $\gamma_{PIB}-\gamma_{PE}$ (mN m^{-1})	γ_{23}, $\gamma_{PIB}-\gamma_{PE}$ (mN m^{-1}) γ_0-lit.	γ_{23}, $\gamma_{PIB}-\gamma_{PE}$ (mN m^{-1}) T_C-lit.	γ_{23}, meas. (mN m^{-1})	Temp. (°C)
PIB1–PE1	0.181, 24.02–27.06	0.124, 26.78–29.42	0.153, 25.43–28.30		170
PIB1–PE2	0.181, 24.02–27.06	0.109, 26.78–29.25	0.144, 25.43–28.21		170
PIB2–PE2	0.161, 25.26–28.19	0.147, 27.38–30.29	0.156, 26.44–29.39	0.58 ± 0.02	150
B8–PE2	0.181, 24.02–27.06			0.49 ± 0.04	170

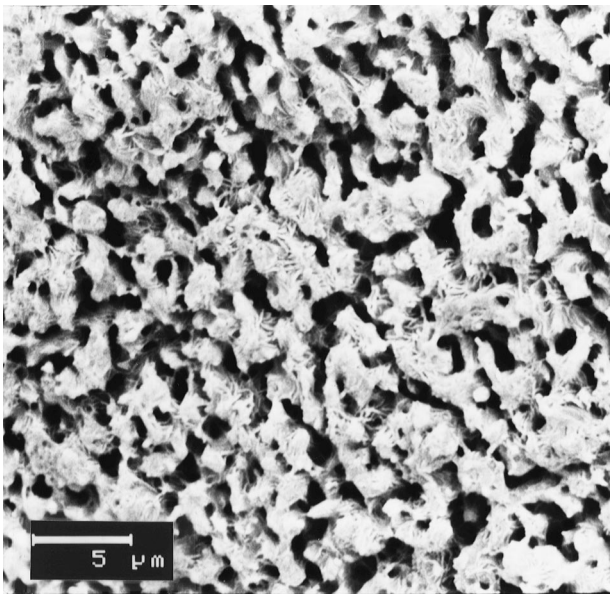

Figure 2 SEM micrograph of a residue of a PIB-extracted cryofracture surface of B1 (PIB1/PE1, 53.6/46.4)

change then a new T_C is calculated. Then in a second step it was assumed that T_C is constant, which gives a new γ_0. Two approximations of the interfacial tension may now be calculated for the modified constants. They are given in columns three and four of *Table 3*. All of these calculated interfacial tensions are very low. To get a direct measurement of γ_{23} we utilized the imbedded disc retraction method[12]. The low viscosities of PE2–PIB2 lead to too rapid retraction of the PE disc at 170°C. Instead, the experiment was run at 150°C and the 15/85 homologous blend of PIB1/PIB2 (B8) was better suited as a matrix at 170°C. These interfacial tensions are much higher than the calculated values, but they are still low compared to other polymer pairs. For example, the interfacial tension of PS/PMMA[12] was found to be 1.1 mN m^{-1} at 210°C and Luciani *et al.*[13] found PS/LDPE and LDPE/PA6 to be 6.4 and 8.9 mN m^{-1}, respectively. The discrepancy between measured and calculated γ_{23} may be caused by inherent errors in the experimental procedure used to determine the surface tensions of the polymers. A further and more fundamental criticism concerns the fact that the harmonic mean approximation (equation (2)) is purely empirical. Results from the imbedded disc retraction method may also suffer from errors, for instance degradation of the PIB by monomer unzipping may have plasticized the polymers leading to an increased retraction rate of the PE disc giving too high γ_{23} values.

The three blends that are close to a volume ratio of unity are displayed in *Figures 2–4* together with B4 in *Figure 3b* that was designed according to equation (1). The coarseness of B1, B3 and B5 increases with decreasing viscosity of one or both components since the micro shear stresses are determined by the macro shear rate that balances the interfacial tension. Such a local increase reduces the viscosity of the extremely shear thinning PE1 and PIB1. Furthermore, B5 in *Figure 4* shows two sub-phases, one PE-enriched and one PE-poor. B2 has an even finer morphology than B1 while B4 in *Figure 3b* lost most of its structural strength upon extraction of the PIB phase, which indicates a non-perfect co-continuous structure. B6 has similar sub-phases to B5 but the PE-poor phase is not as poor.

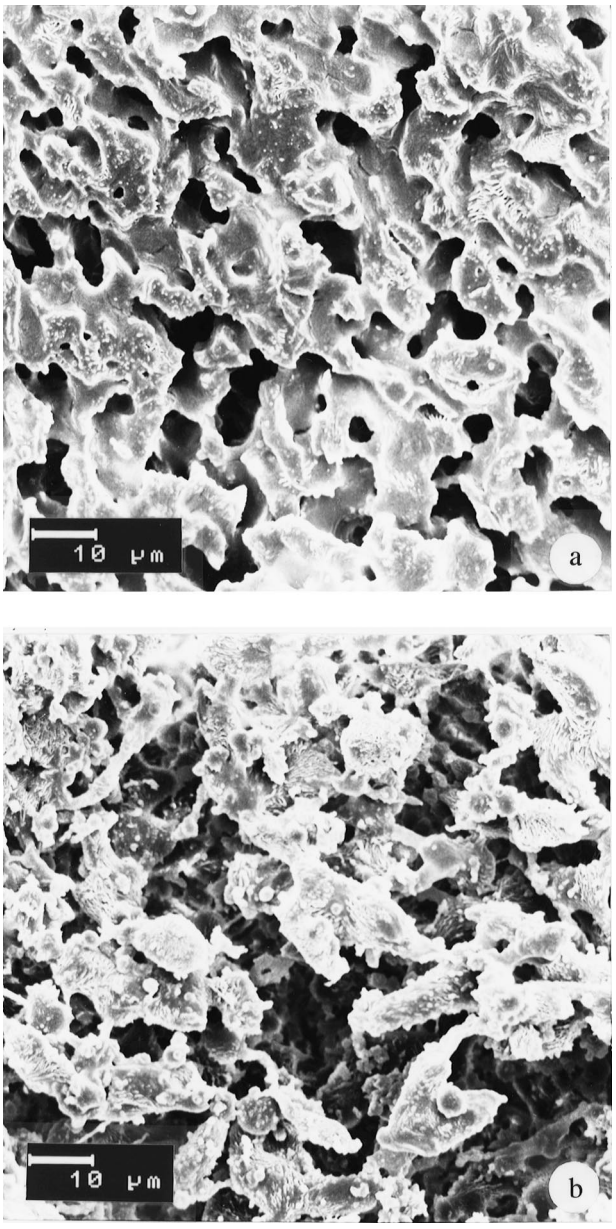

Figure 3 SEM micrographs of residues of PIB-extracted cryofracture surfaces of PIB1/PE2 blends in (a) 53.6/46.4 (B3) and (b) 73.0/27.0 (B4) ratios

For the extracted composite C5, seen in *Figure 5a*, there are many whiskers in the residual high viscosity PE1 phase. The same applies to *Figure 5b* where composite C8 is shown. The difference between them is that the whiskers originated in the PIB1 phase for C5 and in the PE1 phase for C8. The whiskers are almost entirely covered by PE1. C5 has a somewhat coarser phase structure, which may be explained by the surprising fact that the viscosity of the PIB1 phase was slightly but significantly reduced during preparation of the master-batch C1, giving C5 a somewhat higher viscosity ratio than C8. Only C1 of the master-batches C1–C4 showed this indication of degradation.

When the PIB phase is the high viscosity one, as in *Figure 6*, the whiskers seem to have been absorbed exclusively by the PIB1 phase considering all the free and uncovered whiskers. At the higher PIB content, in *Figure 7*, there are no whiskers to be seen, they have all been absorbed by the low viscosity PE2 phase. *Figure 3b* shows that the dispersed PE2 phase is on the very edge of co-continuity since the

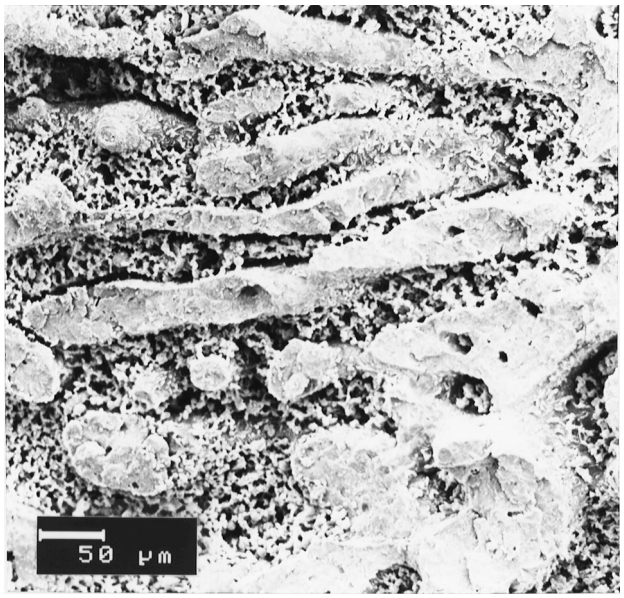

Figure 4 SEM micrograph of a residue of a PIB-extracted cryofracture surface of B5 (PIB2/PE2, 53.6/46.4)

remaining structure is coherent even after the PIB extraction. Pyrolysis of the extracted residue reveals that the PE2 constitutes a continuous phase together with the whiskers. The reasons for this formation are discussed in the rheological section.

When the PE phase again becomes highly viscous, as in composite C17, the whiskers are found in the PE-rich phase. This can be seen in *Figure 8b* which is a close-up of the PE-rich phase in *Figure 8a*. No whiskers can be found in the close-up of the PE-poor phase displayed in *Figure 8c*.

All the hitherto discussed blends and composites had a volume ratio close to one or in agreement with equation (1), i.e. they have all had or been close to co-continuity. For all but the two complementary C11 and C16, the whiskers have been absorbed by the high viscosity phase. To check if this whisker distribution phenomenon was limited to the constraint of co-continuity or if it was of a more general nature, C12 and C14 were compounded to achieve a dispersed high viscosity phase. *Figure 9* clearly shows that the whiskers have been located in the high viscosity PIB1-phase. To sum up, the high viscosity phase always absorbs the whiskers for all the composites C5–C21 that are not explicitly discussed here, except for the two complementary C11 and C16 plus the C7 and C13 that are very difficult to judge.

For a polymer pair with intersecting flow curves, fillers should change environment simply by altering the shear rate provided that the viscous effect is the sole distributing force. Blends of the two PIBs and the PEs produced such intersecting flow curves as seen in *Figure 10*. C22 was prepared from these homologous blends and was sheared in steady rotational shear with cone and plate at 0.1 and 100 s^{-1}. The whisker distributions of these samples were studied by SEM. *Figure 11* clearly shows that the whiskers are found in the PE phase at both shear rates. The only previous experience of PIB as the high viscosity phase was from the PIB1/PE2 blends and composites, which had large viscosity differences, as seen in *Figure 1*. At the current shear rates (0.1 and 100 s^{-1}) of C22 the viscosity ratios were moderately 1.7. Here we define the viscosity ratio as the quotient of the viscosities of the high and low viscosity

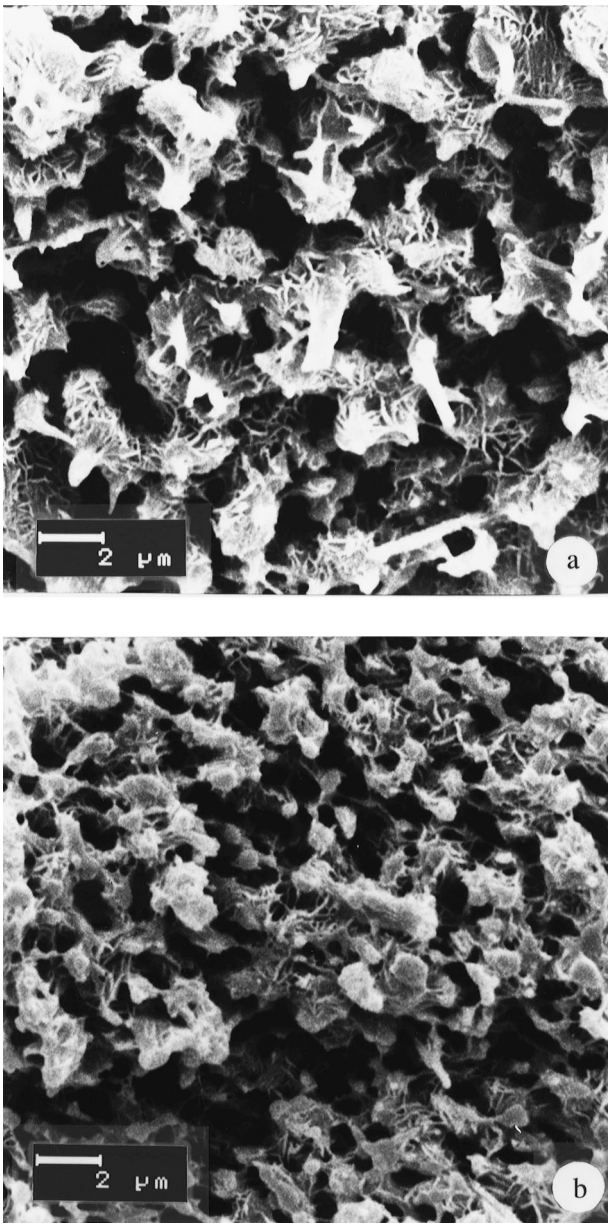

Figure 5 SEM micrographs of residues of PIB-extracted cryofracture surfaces of (a) C5 (PIB1(W)/PE1, 52.6(2.3)/45.1) and the complimentary (b) C8 (PIB1/PE1(W), 52.2/45.5(2.3))

polymers. According to Wu[8] the surface energy of linear PE is somewhat higher than for PIB. The interfacial tension measurements show a difference in surface tension between the components. The rather small interaction strength difference is obviously stronger than the viscous distribution effect, which is suppressed.

To get another measure of the strength of this rheological effect an earlier studied composite[6] was utilised. From that work we learned that PA6 absorbs the whiskers in blends with SAN. Here we chose a SAN with the same acrylonitrile content but with a higher molecular weight to give a viscosity ratio of 30 for the 0.1 s^{-1} shear rate. Despite this large viscosity difference all the whiskers were once again absorbed by the PA6 phase, which constitutes the matrix in *Figure 12*. The dispersed SAN phase was identified by ethylacetate extraction. The anomaly of composite C22 together with C23 shows the relative weakness of this viscous distribution effect. If there are differences in interaction strength they dominate the filler distribution.

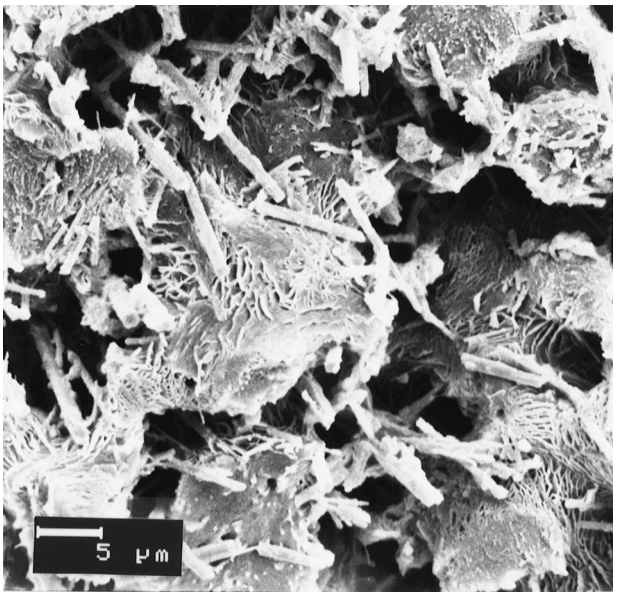

Figure 6 SEM micrograph of a residue of a PIB-extracted cryofracture surface of C10 (PIB1(W)/PE2, 52.6(2.3)/45.1)

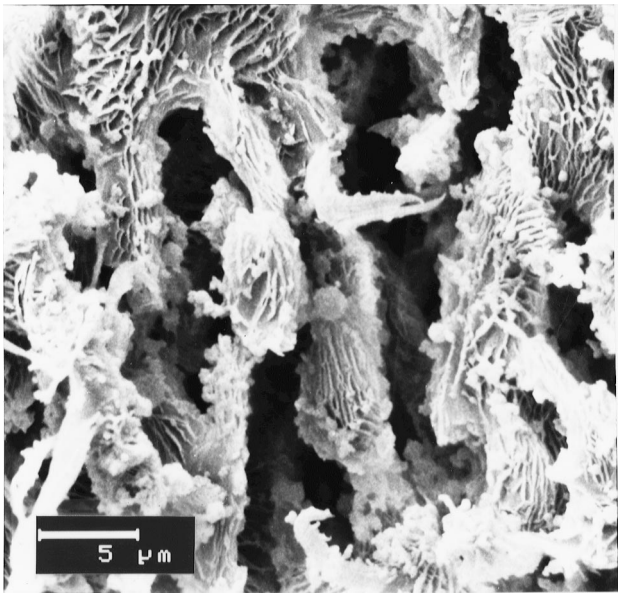

Figure 7 SEM micrograph of a residue of a PIB-extracted cryofracture surface of C16 (PIB1/PE2(W), 67.6/30.9(1.5))

RHEOLOGICAL INTERPRETATION

To understand why a filler is preferentially absorbed by the high viscosity phase in a blend we need a model for the behaviour of the blends. Postulating that the blend/composite configures itself to minimise its dissipative energy (viscosity) during shear sets the fundamental constraint for such models. Much work has been done in the field of rheology of polymer blends[14–20]. Deviation of the viscosity from the rule of mixtures is the general pattern. Many experimental studies have been carried out in capillary rheometers[1,14,17,18]. These are relevant for flow in channels but suffer from the fact that the low viscosity phase tends to encapsulate the high viscosity phase to create a core-shell morphology. For such a morphology the anticipated velocity profile is incorrect and its interpretation

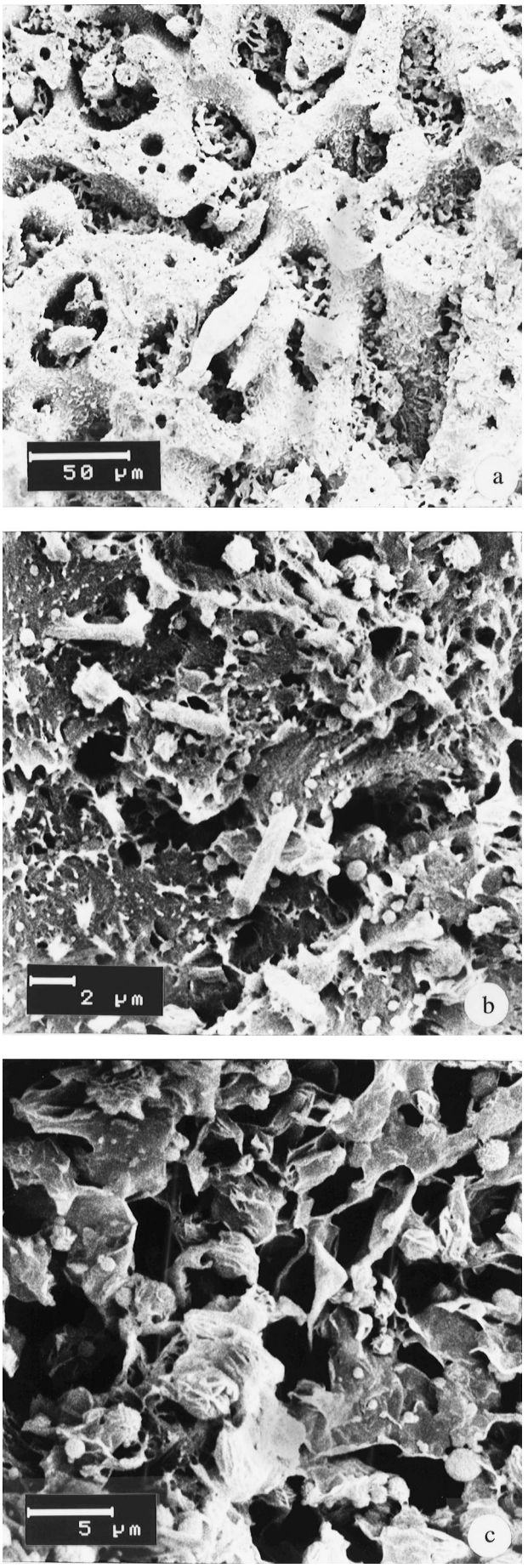

Figure 8 SEM micrographs of a residue of a PIB-extracted cryofracture surface of C17 (PIB2(W)/PE2, 52.6(2.3)/45.1) where (b) and (c) are close-ups of the PE-rich and PE-poor phases seen in (a)

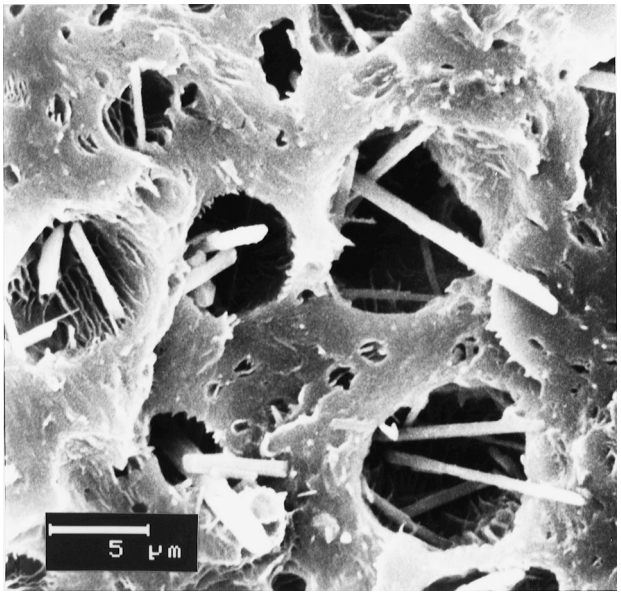

Figure 9 SEM micrograph of a residue of a PIB-extracted cryofracture surface of C12 (PIB1(W)/PE2, 32.8(1.4)/65.8)

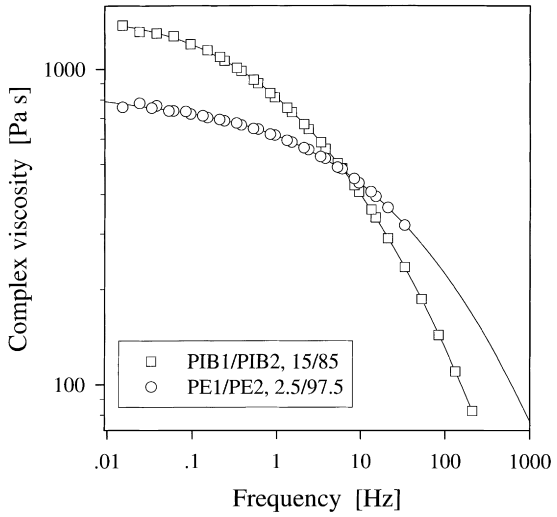

Figure 10 Rheological behaviour from rotational rheometer runs of the homologous blends B7 and B8. The rheometer was run in harmonic mode at 170 and 100°C (curve shifted to 170°C) for B8 and 170 and 140°C (curve shifted to 170°C) for B7

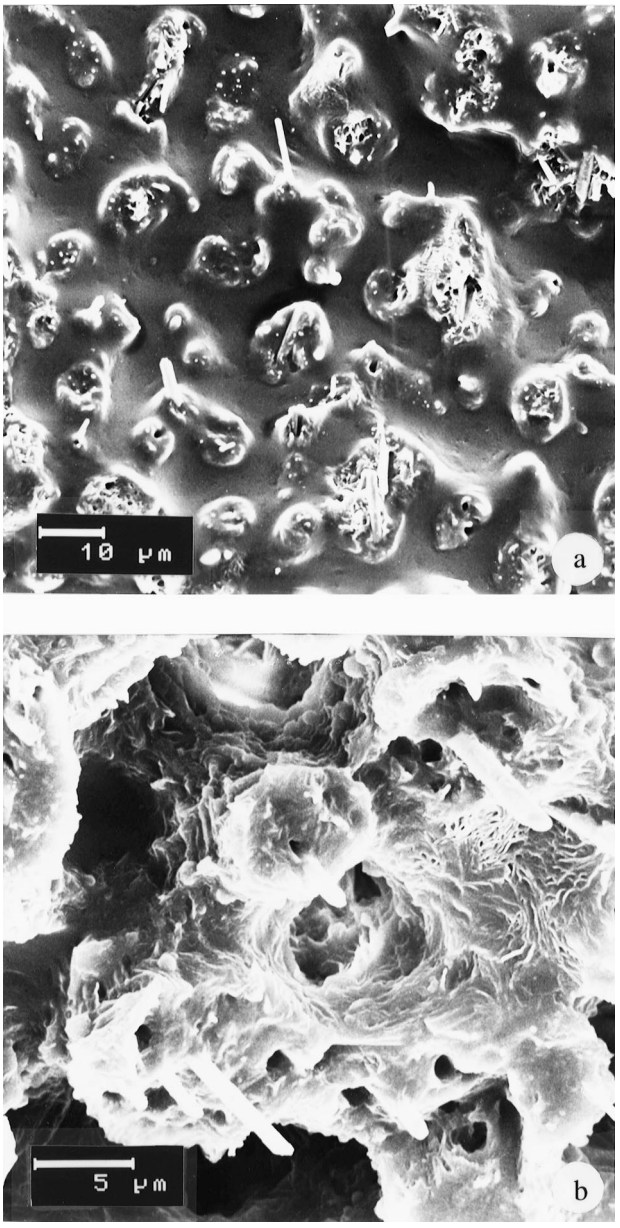

Figure 11 SEM micrographs of cryofracture surfaces of C22 (B8/B7-W, 52.3/45.3-2.4) which have been sheared for (a) 3.1 rad shear angle and 0.1 s^{-1} rate and (b) 790 rad at 100 s^{-1} following PIB extraction

is very precarious. Steady shear with cone and plate offers a more attractive shear mode with a uniform shear rate throughout the sample. This method has been utilized in investigations of the rheology of these blends and composites. Most present models deal with polymer blends where one polymer is suspended in the other. They work neither for co-continuous morphologies nor for compositions in the vicinity of phase inversion. A phase morphology fairly close to a co-continuous structure is the lamellar one which was rheologically characterized by Carriere *et al.*[21]. They showed the applicability of equation (5)

$$\eta = \frac{2\eta_1\eta_2}{\eta_1 + \eta_2} \tag{5}$$

for a two polymer ply with viscosities η_1 and η_2 of two or more layers with volume ratio one. If we consider other volume ratios of the polymers, ϕ_1 and ϕ_2, equation (5) is modified to give:

$$\eta = \frac{\eta_1\eta_2}{\phi_1\eta_2 + (1-\phi_1)\eta_1} \tag{6}$$

If the two fluids are Newtonian this sets the lower limit for the viscosity of the blend. However, as polymers tend to be shear thinning the lower limit can be further reduced especially if the low viscosity component is strongly shear thinning, e.g. blends with a thermotropic liquid crystalline polymer (LCP) phase. The theoretical lower limit is valid when all the deformation takes place in the low viscosity phase, which is given by the viscosity divided by the volume fraction of the low viscosity polymer, i.e. $\eta = \eta_1(\dot{\gamma}/\phi_1)$. In our study of morphologies that are close to co-continuity both phases have to deform.

Figure 13 shows the rheokinetical response to steady shear of blend B3. The compounded blend was heated for approximately 14 min during application and thermal

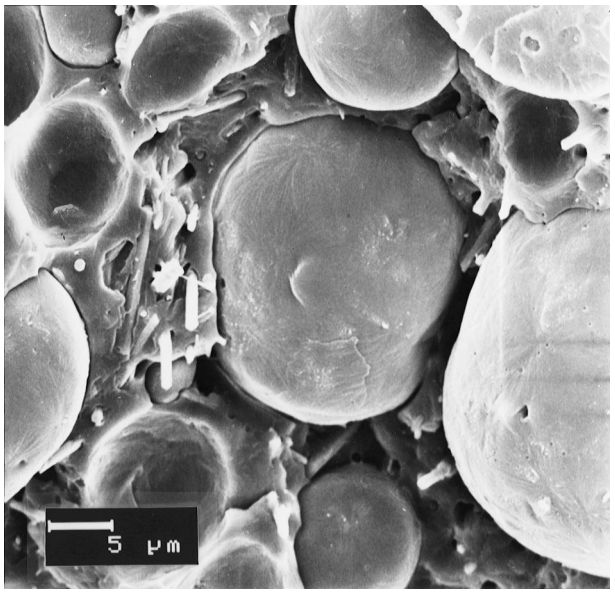

Figure 12 SEM micrograph of a fracture surface of C23 (SAN/PA6-W, 46.4/46.4-7.2 % by weight). The sample comes from a disc that was sheared 3.1 rad at 0.1 s^{-1} and 235°C

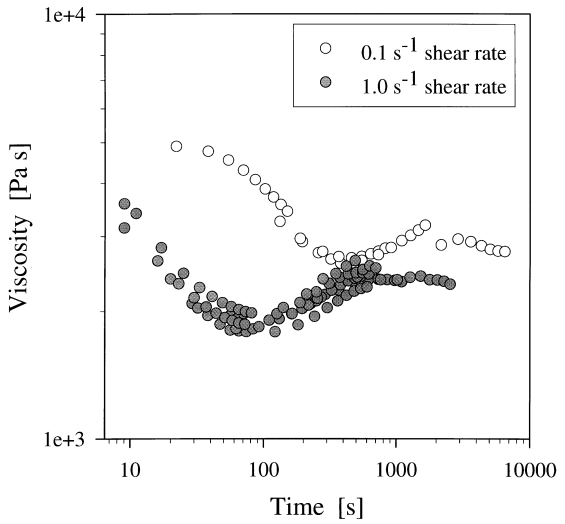

Figure 13 Rheokinetics of blend B3 (PIB1/PE2, 53.6/46.4)

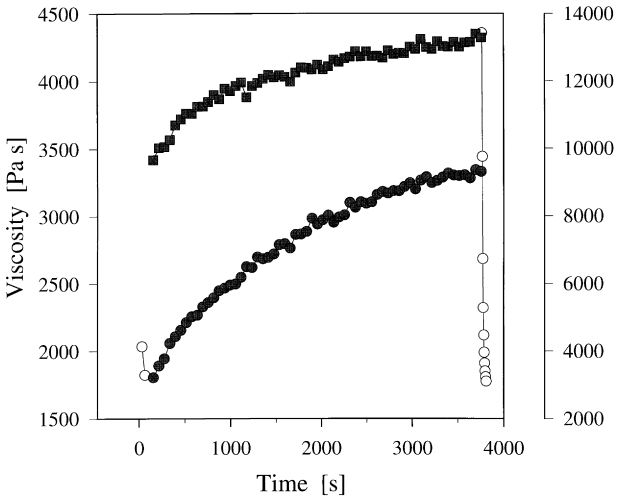

Figure 14 Rheokinetical changes of B3 (PIB1/PE2, 53.6/46.4) first sheared at 1 s^{-1} steady shear for 63 seconds (○), sampled every 31 s, followed by 1 h of harmonic oscillation at 1 Hz and 0.5% strain amplitude where ● symbolises the storage and ■ the loss modulus. The sample was then once again sheared at 1 s^{-1} but now only for 52 s. The temperature was 170°C

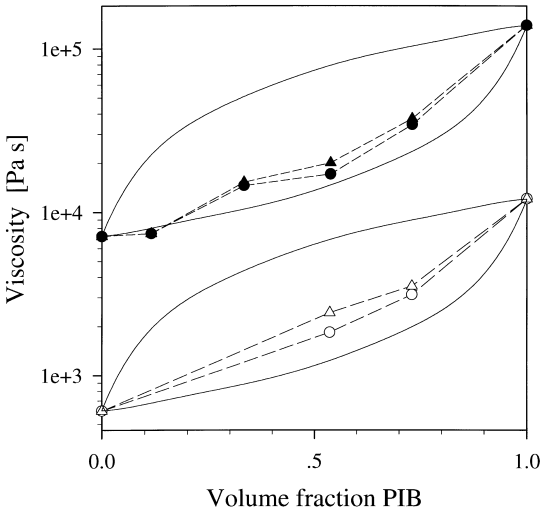

Figure 15 Viscosity of B3–B4, C1, C4 and C10–C16 at 1 s^{-1} shear rate and 170°C. Triangles represent the plateau viscosities and circles the minima. Filled symbols are for the composites and they have been shifted 10 times upward to facilitate interpretation. The upper and lower limiting lines represent the rule of mixtures and equation (6), respectively

conditioning before the shearing started. After approximately 90 s at 1 s^{-1} shear rate the viscosity goes through a minimum and is followed by a build-up to a plateau. The behaviour is similar at the lower shear rate but with a different time scale. We interpret this minimum as rupture of the high viscosity PIB1 phase in the co-continuous structure shown in *Figure 3a*. The discrete PIB-domains are steadily divided until the equilibrium size distribution is reached. Smaller particles tend also to be more spherical, which corresponds to a higher viscosity. This explains the viscosity rise onto the plateau regime. The subsequent stiffening that takes place during harmonic shear at low amplitude in *Figure 14* indicates recovery of the ruptured co-continuous structure. Note the high initial shear viscosity of 4400 Pa s after 1 h of oscillation. It is higher than the initial viscosities seen in *Figure 13*, indicating a more perfect co-continuous structure. The pattern was the same if the sample was left at rest for 1 h instead of oscillating, i.e. the growth was neither caused nor promoted by the oscillation. The viscosities at steady shear for all combinations of PIB1/PE2 fall very close to the lower limit postulated in equation (6). This is especially true for the composites. *Figure 15* shows data obtained from runs such as the one described in *Figure 13*.

A quantitative assessment of the selective absorption is obtained from the following simple model. Einstein's equation for spherical particles of low volume contents combined with equation (6) and the following assumptions provide the tool. Assuming that the filler is absorbed by the low viscosity phase (η_1), one has

$$\eta = \frac{\eta_1\eta_2(1+2.5\phi_w)}{\phi_1\eta_2+(1-\phi_1)\eta_1(1+2.5\phi_w)} \qquad (7a)$$

If the whiskers are absorbed by the high viscosity phase (η_2) equation (7b) is appropriate.

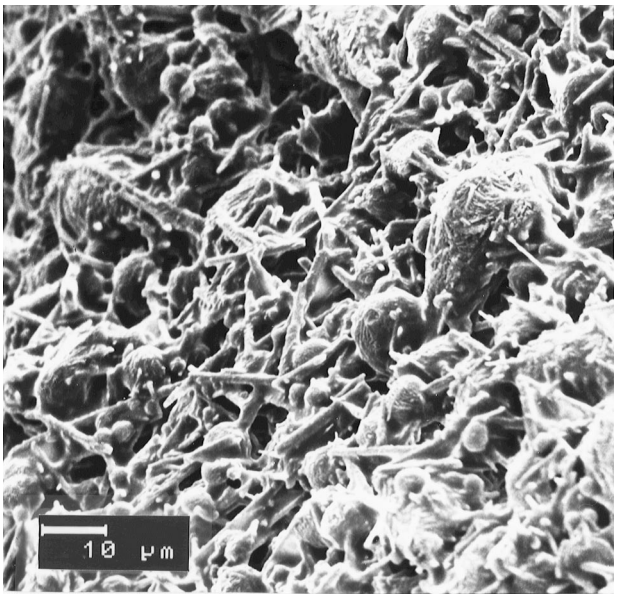

Figure 16 SEM micrograph of a residue of a PIB-extracted cryofracture surface of C19 (PIB2/PE2-W, 66.9/30-3.1)

$$\eta = \frac{\eta_1\eta_2(1+2.5\phi_w)}{\phi_1\eta_2(1+2.5\phi_w)+(1-\phi_1)\eta_1} \qquad (7b)$$

The larger denominator in equation (7b) gives the lower total viscosity of the two.

A similar discussion applies for composites with dispersed high viscosity phases, i.e. C12, C14 and C19. Such a dispersion of discrete spheres was first theoretically treated by Taylor (equation (4.18) in Ref. 14) who extended Einsteiń s equation to account for two Newtonian fluids formulated as

$$\eta = \eta_m\left(1+\frac{5k+2}{2k+2}\phi_d\right) \qquad (8)$$

Here k is the viscosity ratio of the dispersed (d) to the matrix phase (m). Results for composite C12, displayed in *Figure 10*, can serve as an example for the simplified model above. If we calculate the viscosities for the cases where the whiskers are absorbed by either of the PIB1- and PE2-phases, a comparison of the two total viscosities can be made. Using Einsteiń s equation in the same manner as for equations (7a) and (7b), equation (8) gives 945 Pa s for the whiskers in the PIB1-phase for a shear rate of 1 s^{-1}. The calculated viscosity for the whiskers in the PE2-phase is 980 Pa s. Thus a minimization of the dissipative energy for absorption of the whiskers by the high viscosity phase is obtained. However, it should be stressed that this is a rough estimate and a more profound analysis is desirable. For blends of PIB2 and PE2, with viscosity ratio much closer to one, equation (8) indicates absorption by the low viscosity phase. Composite C19 would give 641 Pa s, compared to 731 Pa s if the dispersed PE2-phase had absorbed the whiskers. This prediction is shown to be partly incorrect by the SEM-micrograph in *Figure 16* where the whiskers are covered by a thin PE-layer and large PE-domains still remain, i.e. the PE phase tends to stay dispersed while the slightly higher surface energy of PE governs its whisker coverage. Minimization of the interfacial tension seems to be the strongest distributing criterion. The morphology is also far more complicated than assumed in the calculations. The coherent PIB-extracted sample is yet another example of how the whiskers promote co-continuity.

Among the composites with a low viscosity minor phase (C6, C7, C9, C11, C16, C18 and C21) C6 and C9 seem to create co-continuous structure without any whisker support. C7, C18 and C21 give dispersed low viscosity phases whereas C11 (PIB1(W)/PE2, 70.8(3.1)/26.1) and C16 (PIB1/PE2(W), 67.6/30.9(1.5)) give co-continuous structures. They both fulfill equation (1) fairly well with high viscosity ratios that provide an inherently large potential for viscosity reduction if the PE2 phase serves as a lubricant. The viscosity is minimized for the morphology that maximizes the interfacial area. Hence a disc shaped or fibrillated low viscosity phase explains the synergistic viscosity effect visualized in *Figure 15*. When the PE phases cover the whiskers their domains become more elongated compared to the domain sizes of the pure blend, which clarifies why the filled polymer blends are closer to equation (6) in *Figure 15*. Such elongation of the lubricating phase reduces the viscosity of the composite. The selective absorption by the low viscosity PE phase was confirmed by quantitative weight loss upon PIB extraction of C11 and C16. Furthermore, the slightly higher surface energy of PE contributes to the achieved morphology.

CONCLUSIONS

This work shows that fillers such as aluminium borate whiskers are absorbed by the phase that minimizes the viscosity of PIB/PE blends. The filler is consequently absorbed by the high viscosity phase except when a minority low viscosity phase can become continuous with support from the whiskers. Such a change gives a substantial viscosity reduction of the composite. In blends with polymers interacting about equally strongly with the filler rheologically induced selective absorption should be the general behaviour. This phenomenon must be considered especially for large viscosity ratios, whereas unequal surface interactions govern the filler distribution. These morphological changes may be studied *in situ* as rheokinetical changes during deformation.

ACKNOWLEDGEMENTS

We would like to thank Jean-Luc Roulet who did the interfacial tension measurements. The Swedish National Board for Industrial and Technical Development (NUTEK) is gratefully acknowledged for financial support within the framework of the materials consortium ‘Interfacial Interactions in Polymeric Systems’.

REFERENCES

1. Benderly, D., Siegmann, A. and Narkis, M., *Polymer Comp.*, 1996, **17**(3), 343.
2. Kim, B. K., Kim, M. S. and Kim, K. J., *J. Appl. Polym. Sci.*, 1993, **48**, 1271.
3. Pukánszky, B., Tüdős, F., Kolařik, J. and Lednický, F., *Polymer Comp.*, 1990, **11**(2), 98.
4. Marosi, G., Bertalan, G., Anna, P. and Rusznak, I., *J. Polym. Sci.: Part B: Polym. Phys.*, 1993, **12**(1-2), 33.
5. Persson, A. L. and Schreiber, H. P., submitted to *J. Polym. Sci.: Part B: Polym. Phys.*, 1997, **35**, 2457.
6. Persson, A. L. and Bertilsson, H., *Composite Interfaces*, 1996, **3**(4), 321.
7. Ljungqvist, N., Hjertberg, T., Persson, A. L. and Bertilsson, H., *Composite Interfaces*, 1997, **5**(1), 11.
8. Wu, S., *Polymer Interface and Adhesion*. Marcel Dekker, New York, 1979.
9. Chmutin, I. A., Letyagin, S. V., Schevchenko, V. G. and Ponomarenko, A. T., *Polym. Sci.*, 1994, **36**(4), 576.

10. Bigg, D. M., *Polym. Engng Sci.*, 1979, **19**(16), 1188.
11. Jordhamo, G. M., Manson, J. A. and Sperling, L. H., *Polym. Engng Sci.*, 1986, **26**(8), 517.
12. Rundqvist, T., Cohen, A. and Klason, C., *Rheol. Acta*, 1996, **35**, 458.
13. Luciani, A., Champagne, M. F. and Utracki, L. A., *Polym. Networks Blends*, 1996, **6**(2), 51.
14. Han, C. D., *Multiphase Flow in Polymer Processing*. Academic Press, New York, 1981.
15. Utracki, L. A., in *Rheological Measurement*, ed. A. A. Collyer and D. W. Clegg, Elsevier, London, 1988.
16. Yang, H. H., Han, C. D. and Kim, J. K., *Polymer*, 1994, **35**(7), 1503.
17. Wu, S., *Polym. Engng Sci.*, 1987, **27**(5), 335.
18. Hietaoja, P. T., Holsti-Miettinen, R. M., Seppälä, J. V. and Ikkala, O. T., *J. Appl. Polym. Sci.*, 1994, **54**, 1613.
19. Graebling, D., Muller, R. and Palierne, J. F., *Macromolecules*, 1993, **26**, 320.
20. Mekhilef, N. and Verhoogt, H., *Polymer*, 1996, **37**(18), 4069.
21. Carriere, C. J. and Ramanathan, R., *Polym. Engng Sci.*, 1995, **35**(24), 1979.